inter.noise
HAMBURG 2016

Acoustic characterization of leaks in a pipeline

Jeong-Guon IH[1]; Elmira YADOLLAHI[2]

[1,2] Center for Noise and Vibration Control (NoViC), Department of mechanical Engineering, KAIST, Daejeon, Korea

ABSTRACT

Acoustic reflectometry is applied to detect and characterize the leaks in a long pipeline containing a gas. The inverse algorithm developed for the geoacoustic system having layered media is adopted and modified in reconstructing the sectional impedance along the duct. To separate the incident and reflected waves, which vary during the measurement time span, the three-microphone technique is employed. The measured data are used for the inverse estimation with calculating the spatial distribution of reflection coefficient, determined for each sectional area, which is uniformly located along the duct. The main concerns are the precision of axial leak position, the detectability of very small leak, the applicability to a lengthy duct, and the characterization of the leak size. From the acoustic impedance of sectional area, which is discretely distributed along the duct, a detection criterion to decide the existence of a small leak is suggested. Then, the minimum estimation interval in axial direction is obtained through the statistical data treatment. Experiment is conducted with varying the size and position of leaks. From the experimental results, it is shown that the size and position of leaks can be specified with good precision for a given long duct length.

Keywords: Acoustic reflectometry, Leak detection, Inverse estimation, Small leak, Long pipeline, I-INCE Classification of Subjects Number(s): 26.1, 37.4, 74.6, 76.9

1. INTRODUCTION

Leak in a pipeline in many mechanical services causes various problems related to the mechanical efficiency as well as the environmental problem including the potential hazard. Diagnostic and prognostic of the pipeline for detecting the leak is important, in particular in the early stage of the leak size development. Leak detection methods in current practice are different in the measurement parameters used in the physical or acoustical methods, and also are different for the medium inside pipe. For the liquid-filled pipes, acoustic correlation between two end positions or leakage noise itself inside the pipe are used for the detection (for example, 1,2). For the gas-filled pipes, various non-acoustic methods using the chemical analysis of the gas medium or surrounding solid medium subjected to the infiltration of leakage gas, and the monitoring flow condition itself are suggested (for example, 3,4), and the acoustic methods similar to the liquid-filled pipe case are also suggested (for example, 5-8). In addition, the acoustical method exists that employs the inverse reconstruction of sectional area in a gas-filled duct by manipulating the measured acoustic transfer data (10,11). All the aforementioned methods are promising for the detection of leaks in a pipe. However, the non-acoustical methods are usually slow, and, in most methods, multiple leaks cannot be detected easily. Acoustical methods are not useful for the pipes with bends, and, in particular, the methods using the transient signal experience a difficulty in detecting small or multiple leaks (8-10).

In this study, the geoacoustic algorithm to identify the acoustic characteristics of layers of different soil compositions or to characterize the inhomogeneity of sectional area change is adopted as the main detection theory. In such method, the inverse reconstruction of different layers or sectional areas is based on the identification of impedance distribution, which is facilitated to find the impedance change due to the presence of leaks. By separating the upstream and downstream acoustic waves through the measurement by using the multiple microphone method, the pressure reflection coefficient is precisely determined, and the data is used for the reconstruction of the sectional impedance distribution along the downstream direction (11,12). By comparing the sectional

[1] J.G.Ih@kaist.ac.kr
[2] elmira.yadollahi@kaist.ac.kr; Currently working at SM Instruments Co., Korea

acoustic impedance with and without leak condition, we can identify the location and approximate size of the multiple leaks. The main concerns are the precision of axial leak position, the detectability of very small leak, the applicability to a lengthy duct, and the characterization of the leak size.

2. THEORETICAL BASIS FOR IDENTIFYING THE LEAK CHARACTERISTICS

The algorithm adopted in this work is derived by solving the classical inverse scattering problem in a stratified elastic medium reflecting the seismic waves (12,13). In this geoacoustical method, the semi-infinite elastic ground is composed of a number of stratified elastic layers with equal travel time and homogeneous impedance. In this study, such inverse scattering theory for the seismic wave propagation into the geophysical layers is converted to be used for the inverse reconstruction of the sectional impedance along the axial direction of the gas-filled pipe (14-16). Figure 1 displays the fundamental scheme of pipe sectioning for the application of the theory.

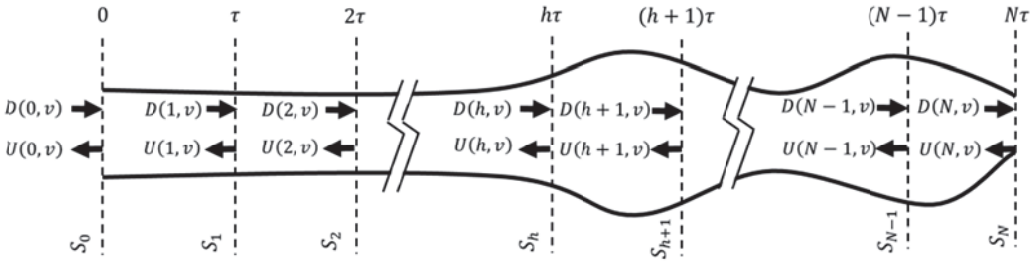

Figure 1 – Subdivided gas layers in a pipe with equal travel time interval τ during the propagation in each pipe segment among the total N segments. Here, *U(h,v)*, *D(h,v)* denotes the upstream and downstream wave, respectively, at the hth segment, *v* is the time-delay constant, and *S* is the sectional area representing the next downstream pipe segment.

In Fig. 1, a pipe is composed of N homogenous finite segments or layers defined by $N+1$ interfaces, of which the spacing of each segment is determined by the equal travel-time interval τ. For each ith layer, the characteristic impedance and sectional area are indexed, so the acoustic impedance for each layer is specified. The numbering of each layer starts from the predetermined upstream position indexed with 0 and ending with the predetermined downstream designated as N. Harmonic plane wave propagation is assumed only. For each ith layer, the interval length is given as Δx_i, which can be defined as $\Delta x_i = c_i \Delta t \ (i = 1, 2, \dots, N)$ using the constant travel time Δt.

For an impulsive wave input to the downstream side at the 0th interface, an infinite sequence of impulses occurring at some multiples of Δt will be generated. Because any reflected wave within a layer should propagate in a double distance of an interval, the time-delay constant v can be defined as $v = e^{j\omega\tau}$, where τ is equal to $2\Delta t$ in the absence of mean flow. Upstream and downstream waves at the hth layer can be used to obtain the waves at the beginning point of the $(h+1)$th layer by using the time-delay constant. Reflection and transmission coefficients between two adjacent layers, r_h and t_h, can be easily derived as

$$r_h = \frac{\rho_h c_h / A_h - \rho_{h+1} c_{h+1} / A_{h+1}}{\rho_h c_h / A_h + \rho_{h+1} c_{h+1} / A_{h+1}}, \tag{1}$$

$$t_h = (1 - r_h{}^2)^{1/2}. \tag{2}$$

Equation (1) becomes a function of sectional areas only when the gas temperature does not change during the propagation. A transfer matrix between two adjacent layers in tandem can be written as

$$\begin{bmatrix} D(h,v) \\ U(h,v) \end{bmatrix} = \frac{1}{\sqrt{v}\, t_h} \begin{bmatrix} v & r_h v \\ r_h & 1 \end{bmatrix} \begin{bmatrix} D(h+1,v) \\ U(h+1,v) \end{bmatrix} \ (h = 0, 1, \dots, N). \tag{3}$$

Then, the overall transfer matrix can be obtained as

$$\begin{bmatrix} D(0,v) \\ U(0,v) \end{bmatrix} = \frac{1}{v^{\frac{h+1}{2}} \prod_{i=0}^{h} t_h} \begin{bmatrix} v^{h+1} F\left(h, \frac{1}{v}\right) & v^{h+1} G\left(h, \frac{1}{v}\right) \\ G(h,v) & F(h,v) \end{bmatrix} \begin{bmatrix} D(h+1,v) \\ U(h+1,v) \end{bmatrix}. \tag{4}$$

By using recursive polynomials of $F(h,v)$ and $G(h,v)$ $(h = 1, 2, \dots, N)$ and initial values of them (14), and also substituting boundary values, the following reflection coefficient can be expressed as a function of travel time:

$$r_{h+1} = \frac{R_{h+1} + F_1(h) R_h + F_2(h) R_{h-1} + \cdots + r_0 r_h R_1}{\prod_{i=0}^{h} (1 - r_i^2)}, \tag{5}$$

where R_h is the measured impulse response at each layer. The impedance ratio q_h between two adjacent interfaces can be obtained as

$$q_h \equiv \frac{Z_h / A_h}{Z_{h-1} / A_{h-1}} = \frac{1 + r_{h-1}}{1 - r_{h-1}} \equiv |q_h| e^{-j\phi(q_h)}. \tag{6}$$

Here, Z_h and Z_{h-1} imply the acoustic impedance of the hth and $(h-1)$th layer, respectively. Because the acoustic impedance at the section of the first interface is known or assumed to be a constant, the acoustic impedance of all layers can be reconstructed. The reconstructed acoustic impedance for each layer can be expressed as

$$Z_h = \prod_{i=0}^{h} \frac{1 + r_i}{1 - r_i} Z_0 A_h / A_0 \equiv |Z_h| e^{-j\phi(q_h)}. \tag{7}$$

Leak localization can be conducted by using the magnitude and/or phase of the reconstructed impedance ratio q_h, or the reconstructed acoustic impedance Z_h. Actually, the difference of one of these parameters from the initially measured data without any leak or with initial amount of leak can be used to identify the leak characteristics.

3. EXPERIMENTAL SETUP

A flexible PVC pipe of circular cross section with a total length of 31 m is prepared for the test. The external and internal diameters of the pipe are 0.1 m and 0.092 m, respectively. The pipe is spirally wound to accommodate the long pipe in a limited space. It is assumed that the pipe curvature has a negligibly small effect in sound propagation if the frequency range of interest is far below the cutoff frequency of the first transverse mode, in this case, 2.18 kHz (17). The sound reflection coefficient is estimated by separating the incident and reflected traveling waves from the measured data by using multiple microphone technique (18). In the measurement, 1/4″ microphones (B&K type 4939) with 0.1 m spacing are flush mounted in the pipe. This microphone spacing lets the frequency range of interest to be between 200 Hz – 1.4 kHz. The sine swept signal for a range of 100 Hz - 1.7 kHz with 1 kHz sweeping rate is fed to a compression driver sound source though a power amplifier (Sherwood R-807 a0073). To reduce the strong sound reflection from the far end of the pipe, a 1 m long fiberglass is filled in. Along the pipe, 7 different locations are selected for placing the leaks. At each location, 3 connecting pipes having circular leaks with different diameters of 0.001, 0.002, and 0.003 m are installed, respectively, for the leakage detection test.

4. TEST RESULTS AND DISCUSSION

Before conducting the experiments with applied leak in the pipe, the impedance ratio q_h and the acoustic impedance Z_h are measured for the pipe without any leak to obtain the reference data for comparison. Because the magnitudes of the measured parameters are fluctuating along the pipe, the data are statistically treated to obtain the statistical probability with 95% and 99% confidence.

4.1 Detection and Localization of a Leak

To detect a leak using each parameter, either magnitude or phase or both of q_h or Z_h can be used.

Figure 2 shows the variation of magnitude and phase of the reconstructed impedance ratio, estimated in the spatial range of a leak position as an example. Existence of a leak and its position can be identified from a transition point from a peak to a trough in the magnitude curve, as designated by $(x_m, 0)$; meanwhile, a simple peak in the phase curve, designated by $(x_c, \phi(q_c))$, indicates the existence of a leak.

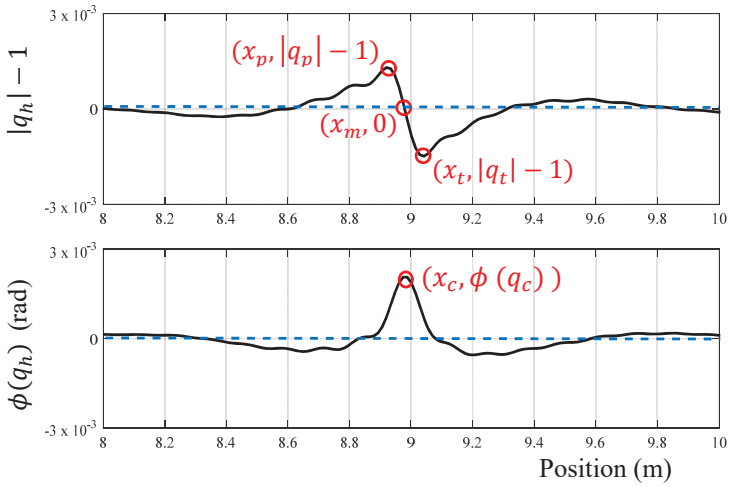

Figure 2 – Variation of magnitude and phase curves of the reconstructed impedance ratio showing the peak and trough fluctuation due to the presence of a leak at x_l =9 m.

Figure 3 shows the magnitude and phase plots of the reconstructed acoustic impedance, estimated in the spatial range of a leak position, as an example. Existence of a leak and its position can be identified from a simple peak in the magnitude curve, as designated by $(x_c, |Z_c|)$; meanwhile, a transition point from a peak to a trough in the phase curve, designated by $(x_m, 0)$, indicates the existence of a leak.

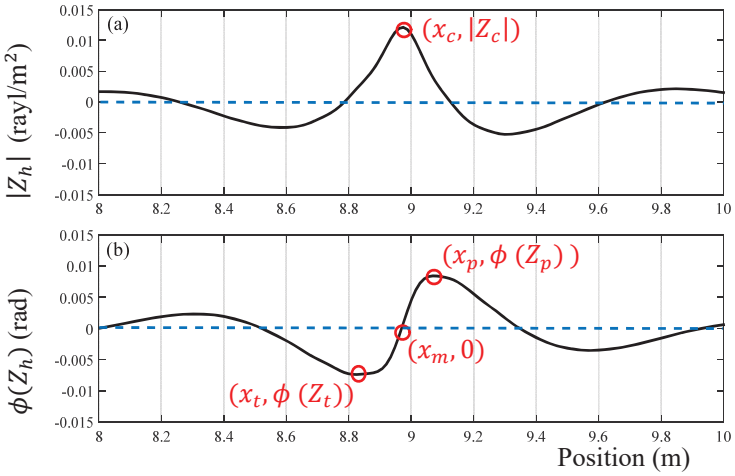

Figure 3 – Variation of magnitude and phase curves of the reconstructed acoustic impedance showing the peak and trough fluctuation due to the presence of a leak at x_l =9 m.

The error in localizing the leak position is influenced from the spatial resolution dx in the measurement and estimation. Figure 4 illustrates the change of detection parameter, in this case the phase of the reconstructed acoustic impedance, with the leak position. One can see that the phase of acoustic impedance peak diminishes with increasing distance from the source, but, even at a far distance like x_l=27.6 m, the leak position is yet clearly localized with a very good probability.

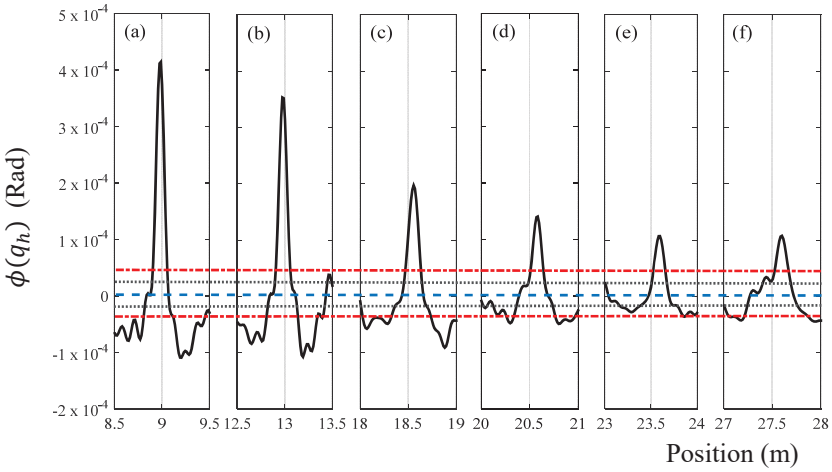

Figure 4 – Estimated phase of the impedance ratio for detecting a leak with 1 mm in diameter located at six different locations x_l; – – –, mean; ·····, 95% confidence interval; – · – · –, 99% confidence interval. (a) $x_l = 9$ m, (b) $x_l = 13$ m, (c) $x_l = 18.6$ m, (d) $x_l = 20.6$ m, (e) $x_l = 23.6$ m, (f) $x_l = 27.6$ m.

4.2 Detectable Leak Size

As discussed in the foregoing section, the spatial fluctuation of the reconstructed acoustic parameters can be used for determining the existence of the leak at a location. When the leak is fixed at an arbitrary position, we varied the size of the leak to investigate its effect on the change of the characteristics of such acoustic parameters. In the experiment, 3 different leak sizes of 0.001, 0.002, and 0.003 mm in diameter are varied at each of 7 different locations in the pipe. Figure 5 depicts the change in the phase of impedance ratio $\phi(q_h)$ with this experiment, exhibiting that the amount of fluctuation in $\phi(q_h)$ follows the size of the leak even though the absolute magnitude of it diminished with the increase of the distance of leak position from the source. Consequently, if we somehow establish an empirical model to correlate the fluctuation magnitude with the distance or signal-to-noise ratio, the size of the leak might be determined from the model.

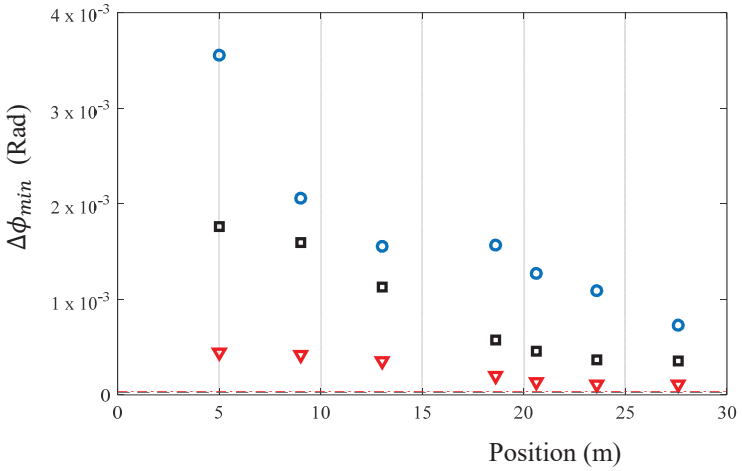

Figure 5 – Change in the phase of impedance ratio q with respect to the different leak positions and different leak diameter: ▽, 1 mm; □, 2 mm; ○, 3 mm, – · – · –, 95% confidence range.

Figure 6 shows a nomogram style plot that can determine the size of a leak at a specific position in the pipe. The three-dimensional surface is generated by implementing a second order polynomial interpolation function, which is applied to the additional experimental data with varying the size from 0.0005 m to 0.004 m. The interpolation is made with 0.0005 m step in leak size, in which a leak of 0.0005 m in diameter is the smallest leak that can be detected in this experiment.

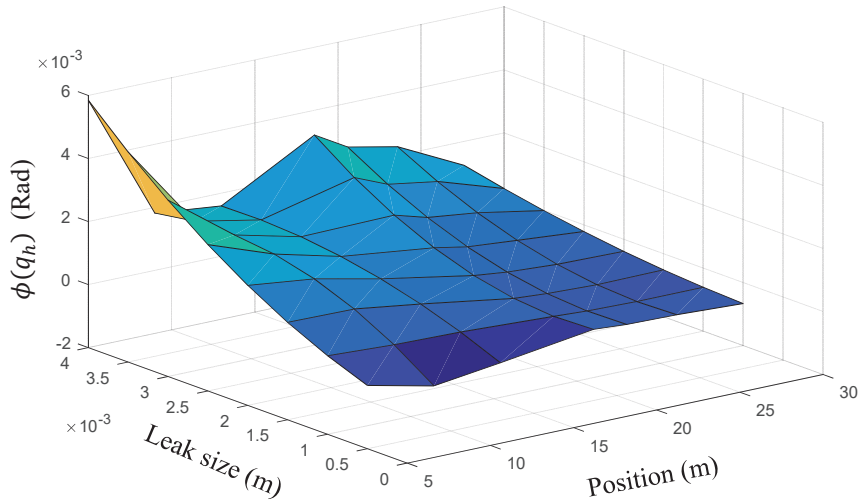

Figure 6 – Three-dimensional interpolated surface plot of the change in the estimated phase of impedance ratio as functions of leak size and position. By using this plot, one can determine the leak size with a resolution of 0.0005 m in diameter at a specific position of that leak.

5. CONCLUSIONS

An experimental and theoretical method for the detection, localization, and size estimation of a leak within a pipeline has been studied using the acoustic reflectometry adopting the multiple microphone technique and the inverse reconstruction of the acoustic impedance distribution along the pipe axis. Study focus is the precision of the localization and the size determination in a long pipe. The existence of a leak in a long pipe or leak in a small size is related with the resultant signal-to-noise ratio of the measured reflected wave amplitude, and a statistical approach is employed for the decision making. In this work, if the magnitude of the phase of impedance ratio is larger than $\pm 3.5 \times 10^{-5}$ *rad* considering a 99% confidence interval, the existence of a leak is confirmed. Similar criterion is found as the detection criteria in using the magnitude of the reconstructed acoustic impedance. The maximum error in leak localization is less than 0.04 m in dealing with the total pipe length of $28\,m$ that corresponds to the 3 discrete sections in the estimation. The smallest detectable leak has 0.5 mm in diameter. The study has been conducted under the assumption that the leak is a circular hole in shape. For the other leaks in the shapes of straight or curved slits, a further study is needed if the present method is also applicable. Although the theoretical formulation has a provision in dealing with the temperature change along the pipe, the change in medium temperature is not tested, and this feature is also left for the further study.

ACKNOWLEDGEMENTS

This work was partially supported by the BK21 Plus Project and the NRF grant (2010-0028680).

REFERENCES

1. Hunaidi O, Chu WT. Acoustical characteristics of leak signals in plastic water distribution pipes. Appl. Acoust. 1999; 58: 235-254.
2. Kurtz DW. Developments in free-swimming acoustic leak detection systems for water transmission pipelines. Proc. ASCE Conf. 2006; 25: 626–632.
3. Sperl J. System pinpoints leaks on point arguello offshore line. Oil Gas J. 1991; 89: 47-52.
4. Olsen MK, Bose JR. TAPS's leak detection seeks greater precision. Oil Gas J. 1993; 91: 43-47.
5. Watanabe K, Matsukawa S, Yukawa H, Himmelblau DM. Detection and location of a leak in a gas-transport pipeline by a new acoustic method. AlChE J. 1986; 32: 1690-1702.
6. Hough JE. Leak testing of pipelines uses pressure and acoustic velocity. Oil Gas J. 1988; 86: 35-41.
7. Ivetic M. Practical implications of using induced transients for leak detection. J. Urban and Env. Eng.

2007; 1: 36– 43.
8. Yunus U, Tsunasaki M, He Y, Kominami M, Yamashita K. Detection of leak location in a pipeline by acoustic signal. IEICE Transactions on Fundamentals of Electronics, Comm. Comp. Sc. 2008; 91: 2053–2061.
9. Sharp DB, Campbell DM. Leak detection in pipes using acoustic pulse reflectometry. Acustica 1997; 83: 560-566.
10. Papadopoulou KA, Shamout MN, Lennox B, Mackay D, Taylor AR, Turner JT, Wang X. An evaluation of acoustic reflectometry for leakage and blockage detection. Proc. IMechE Part C 2008; 222: 959-966.
11. Schroeder MR. Determination of the geometry of the human vocal-tract by acoustical measurements. J. Acoust. Soc. Am. 1967; 41: 1002-1010.
12. Sondhi MM, Resnick JR. The inverse problem for the vocal tract: numerical methods, acoustical experiments, and speech synthesis. J. Acoust. Soc. Am. 1983; 73: 985-1002.
13. Goupillaud P. An approach to inverse filtering of near-surface layer effects from seismic records. Geophysics; 1961; 26: 754-760.
14. Ware JA, Aki K. Continuous and discrete inverse-scattering problems in a stratified elastic medium. I. plane waves at normal incidence. J. Acoust. Soc. Am. 1968; 45: 911-921.
15. Ning W, JunXuan L, Sadayuki U. Goupillaud inverse problem with arbitrary input. J. Opt. Soc. Am. 1997; 101: 3255-3260.
16. Kim HJ, Ih JG, Lee JS. Inverse acoustical measurement of the sectional area in non-uniform ducts. Proc. ICSV. 2001; 1601-1606.
17. Kim JT, Ih JG. Transfer matrix of curved duct bends and sound attenuation in curved expansion chambers. Appl. Acoust. 1999; 297-309.
18. Jang SH, Ih JG. On the multiple microphone method for measuring in-duct acoustic properties in the presence of mean flow. J. Acoust. Soc. Am. 1998; 103: 1520-1526.